Bipolar resistive switching in $BiFe_{0.95}Zn_{0.05}O_3$ films*

Yuan Xue-Yong(袁学勇)[a], Luo Li-Rong(罗丽荣)[b], Wu Di(吴 迪)[c], and Xu Qing-Yu(徐庆宇)[a]†

[a] *Department of Physics, Southeast University, Nanjing* 211189, *and Key Laboratory of MEMS of the Ministry of Education, Southeast University, Nanjing* 210096, *China*

[b] *School of Materials Science and Technology, Nanjing University of Aeronautics and Astronautics, Nanjing* 210016, *China*

[c] *Department of Materials Science and Engineering, Nanjing University, Nanjing* 210008, *China*

(Received 30 March 2013; revised manuscript received 10 May 2013)

Bipolar resistive switching is studied in $BiFe_{0.95}Zn_{0.05}O_3$ films prepared by pulsed laser deposition on (001) $SrTiO_3$ substrate, with $LaNiO_3$ as the bottom electrode, and Pt as the top electrode. Multiple steps of resistance change are observed in the resistive switching process with a slow voltage sweep, indicating the formation/rupture of multiple conductive filaments. A resistive ratio of the high resistance state (HRS) to the low resistance state (LRS) of over three orders of magnitude is observed. Furthermore, the conduction mechanism is confirmed to be space-charge-limited conduction with the Schottky emission at the interface with the top Pt electrodes in the HRS, and Ohmic in the LRS. Impedance spectroscopy demonstrates a conductive ferroelectric/interfacial dielectric 2-layer structure, and the formation/rupture of the conductive filaments mainly occurs at the interfacial dielectric layer close to the top Pt electrodes.

Keywords: multiferroics, resistive switching

PACS: 77.55.Nv, 72.20.Ht, 73.50.Fq **DOI:** 10.1088/1674-1056/22/10/107702

1. Introduction

Resistance random access memory (RRAM)[1,2] based on resistive switching (RS) is deemed to be the most promising category of next-generation nonvolatile memory and has attracted much interest recently due to its simple structure, rapid write/erase operation, low power consumption, and high-density integration.[3–5] Furthermore, RS is widely observed in transition metal oxides and perovskite oxides, such as NiO,[6] TiO_2,[7] (PrCa)MnO_3,[8] and $SrTiO_3$.[9] Although RS phenomena have been studied for decades, the mechanism is still not clearly identified. Various mechanisms have been proposed to explain the reversible switching of resistance state, including formation/rupture of conductive filaments,[10,11] Schottky barriers at interfaces,[12,13] etc.

As the only single phase multiferroic material above room temperature, $BiFeO_3$ (BFO) has attracted great attention due to its potential application in spintronics, photoelectronics.[14–16] The RS effect was first observed by Yang in Ca-doped $BiFeO_3$ epitaxial film,[17] and later was also observed in $BiFeO_3$ films, and different models have been applied to explain the physical origin of this behavior. Bipolar resistive switching (BRS) has been observed by Shuai, which he attributed to the electric field-induced carrier trapping and detrapping.[18] Li attributed the BRS to the formation/rupture of the nanoscale metal filaments due to the diffusion of the top electrodes under the bias voltage.[19] Yin attributed the BRS to the formation/rupture of the conductive paths formed by the oxygen vacancies.[20] Wang reported large ferroelectric resistive switching and the observation that the forward direction of rectifying current can be reversed by polarization — this was explained by the polarization-modulated Schottky-like barriers.[21] In this paper, we report the BRS in $BiFe_{0.95}Zn0_{0.05}O_3$ (BFZO) films, and impedance spectroscopy has been employed to understand the BRS mechanism.

2. Experimental details

BFZO films were prepared by pulsed laser deposition (PLD) with a ceramic target $Bi_{1.05}Fe_{0.95}Zn_{0.05}O_3$ (5% excess Bi was introduced to compensate for volatile loss). Zn was incorporated to decrease the leakage current.[22,23] The detailed preparation process has been described before.[24,25] As the bottom electrode and buffer layer, an $LaNiO_3$ (LNO) (30-nm thick) was first deposited on (001) $SrTiO_3$ (STO) substrate at 850 °C under oxygen pressure of 20 Pa. Then the BFZO film (about 80 nm) was deposited at 700 °C under oxygen pressure of 2 Pa. After deposition, the heterostructure was annealed at 550 °C for 30 minutes and then cooled down to room temperature in an oxygen pressure of 1×10^5 Pa. Round Pt top electrodes of 100-μm diameter were deposited on the films through a shadow mask. The structure of the film was examined by X-ray diffraction (XRD, Rigaku SmartLab3) with Cu Kα radiation. The electrical measurements were carried out

*Project supported by the National Natural Science Foundation of China (Grant No. 51172044), the Natural Science Foundation of Jiangsu Province of China (Grant No. BK2011617), the National Key Project for Basic Research of China (Grant No. 2010CB923404), the 333 Project of Jiangsu Province, by NCET-09-0296, the Scientific Research Foundation for Returned Overseas Chinese Scholars, the State Education Ministry, and Southeast University (Grant No. Seujq201106).

†Corresponding author. E-mail: xuqingyu@seu.edu.cn

© 2013 Chinese Physical Society and IOP Publishing Ltd

using a Keithley 2400 SourceMeter and 2182A NanovoltMeter at room temperature. During the measurements, the bias is defined as positive when the current flows from the LNO bottom electrode to the Pt top electrode. Complex impedance measurements were performed in the frequency range from 40 Hz to 110 MHz at room temperature using an impedance analyzer (Agilent 4294A).

3. Results and discussion

The XRD pattern of BFZO film is shown in Fig. 1. All the peaks can be indexed to a pseudo-cubic structure with only (00n) peaks observed, which demonstrates a highly preferred orientation of BFZO film along the c axis. The small diffraction peak marked by an asterisk is from the STO substrate. The (00n) peaks of STO and LNO are located at the right of BFZO, for they have smaller pseudo-cubic c lattice constants (BFO: 3.96 Å,[26] STO: 3.91 Å,[27] LNO: 3.84 Å[28]).

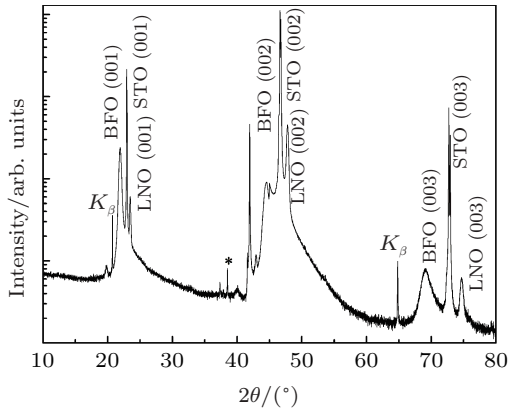


Fig. 1. XRD patterns of STO/LNO/BFZO.

Figure 2(a) shows the I–V curves obtained under dc voltage sweep mode with 30 mV/step. The schematic diagram of the STO/LNO/BFZO/Pt device structure is illustrated in the left bottom inset of Fig. 2(a). As shown in Fig. 2(a), the forming was achieved at a voltage of 2.31 V. After the initial forming process, a typical BRS can be observed in the BFZO film. When a positive voltage is applied on the LNO bottom electrode, the resistance shows an abrupt decrease from the high resistance state (HRS) to the low resistance state (LRS) (defined as SET process) at 1.62 V, and the current becomes nearly two orders of magnitude larger, protected by the 1 mA compliance current. When negative voltage is applied, the resistance switches back from LRS to HRS at −1.16 V (defined as RESET process). As illustrated in the picture, the electric currents in the HRS in the following SET processes are much larger than those in the forming process and the switching voltages in the SET processes are lower than those in the forming process. (We repeated measurements of the I–V curves under the same conditions another 10 times, and the SET voltage was never more than 1.92 V.) The electroforming process generates defects inside the BFZO layer, mostly by the thermally assisted electromigration of oxygen ions.[29] According to the filament model,[30,31] the oxygen vacancies are aligned to form tiny conductive filaments under the electric field, leading to the transition to the LRS during the forming process. Even when the LRS is transformed to the HRS, fragmented or disconnected filaments exist in the BFZO film due to the limited migration of the oxygen ions in the film; consequently the resistance of the HRS of the devices is always much lower than that of the as-made cells.[29] Furthermore, the RESET process is not as rapid as the SET process — it shows gradual change with multiple steps. We measured the I–V hysteresis curves several times to check the reproducibility. Similar multistep switching behavior has been observed in the RRAM devices and was explained by the formation of multiple conductive filaments.[32,33] We also performed statistics of SET/RESET voltage with different cells (not shown here). Our device shows stable resistive switching behavior, the SET voltage was from 1.16 V to 2.02 V and RESET voltage varied

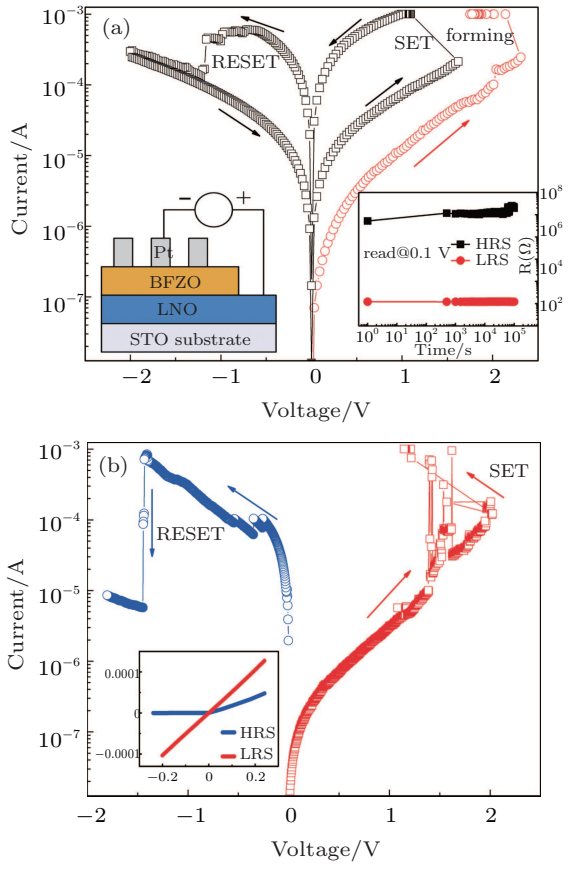


Fig. 2. (color online) (a) The typical I–V characteristics of the LNO/BFZO/Pt structure using a voltage sweeping rate of 30 mV/step. Left bottom inset shows the schematic device structure; right bottom inset shows retention of the HRS and LRS with reading voltage of 0.1 V. (b) I–V characteristics using a voltage sweeping rate of 3 mV/step. Inset is the I–V curves with voltage sweeping from −0.2 V to +0.2 V.

from −1.04 V to −1.60 V. The retention property of our device measured with 0.1 V at room temperature is shown in the right bottom inset of Fig. 2(a). As can be seen, up to 10^5 s, resistance in both the HRS and LRS shows little deterioration and the resistance ratio of HRS/LRS is around 10^3 without degradation.

In order to explore the underlying physics in our device further, we used the dc voltage sweep mode with 3 mV/step, and the *I*–*V* curves are shown in Fig. 2(b). Interestingly, this time the SET process also shows a stepwise switching phenomenon, the SET and RESET voltage were 2.00 V and −1.43 V, respectively. An *I*–*V* sweep between −0.2 V and +0.2 V was performed in the LRS and HRS, as shown in the inset of Fig. 2(b). Clear rectifying characteristics were observed in the HRS, suggesting the formation of a Schottky barrier. Generally, the rectifying behavior comes from a p–n junction or a metal–semiconductor Schottky-like junction due to the energy barrier at the interface. The work function of LNO is 4.5 eV,[34] Pt is 5.3 eV, and BFO can be taken as 4.7 eV.[35] In addition, the BFZO/LNO interface is an epitaxial contact, whereas the Pt/BFO interface is a nonepitaxial contact. The interfacial layer formed at the nonepitaxial Pt/BFO interface may be much thicker than the one formed at the epitaxial BFO/LNO interface, which shows a larger contact resistance. Therefore, a Schottky junction is more likely to be formed at the Pt/BFZO interface; this has been confirmed experimentally by Tsurumaki.[36]

Figures 3(a) and 3(b) show the *I*–*V* curve in the positive and negative voltage regions, which are plotted in log–log scale. As illustrated in the figure, it is clear that the slope of LRS and HRS in low field is close to 1, which can be attributed to Ohmic behavior. As for the high electric field in HRS, it is a bit more complicated to determine the conduction mechanism. The classical nonlinear conduction mechanisms for $BiFeO_3$ mainly include space-charge-limited conduction (SCLC), Schottky emission, and Poole–Frenkel (PF) emission.[37] The current density for SCLC can be expressed as[37,38]

$$J_{\mathrm{SCLC}} = \frac{9\mu\varepsilon_0 K}{8}\frac{V^2}{d^3}, \tag{1}$$

where μ represents the carrier mobility. According to Eq. (1), the plots of $\log(I)$ versus $\log(V)$ should show a linear behavior with a slope of 2. As shown in Figs. 3(a) and 3(b), the slopes in high electric field are 1.88 and 1.76, respectively. This suggests the dominant conduction mechanism in the high voltage region is SCLC. However, the slight deviation of the slope from 2 might be due to deep-level traps,[39,40] and there is contribution from another conduction mechanism.

The Schottky barrier has been confirmed by the rectifying *I*–*V* curve in the HRS. For the Schottky emission, which arises from a difference in Fermi level between metal and semiconductor, the current density is[37]

$$J_{\mathrm{S}} = AT^2 \exp - \left[\frac{\phi}{k_{\mathrm{B}}T} - \frac{1}{k_{\mathrm{B}}T}\left(\frac{q^3 U}{4\pi\varepsilon_0 K d}\right)^{1/2}\right], \tag{2}$$

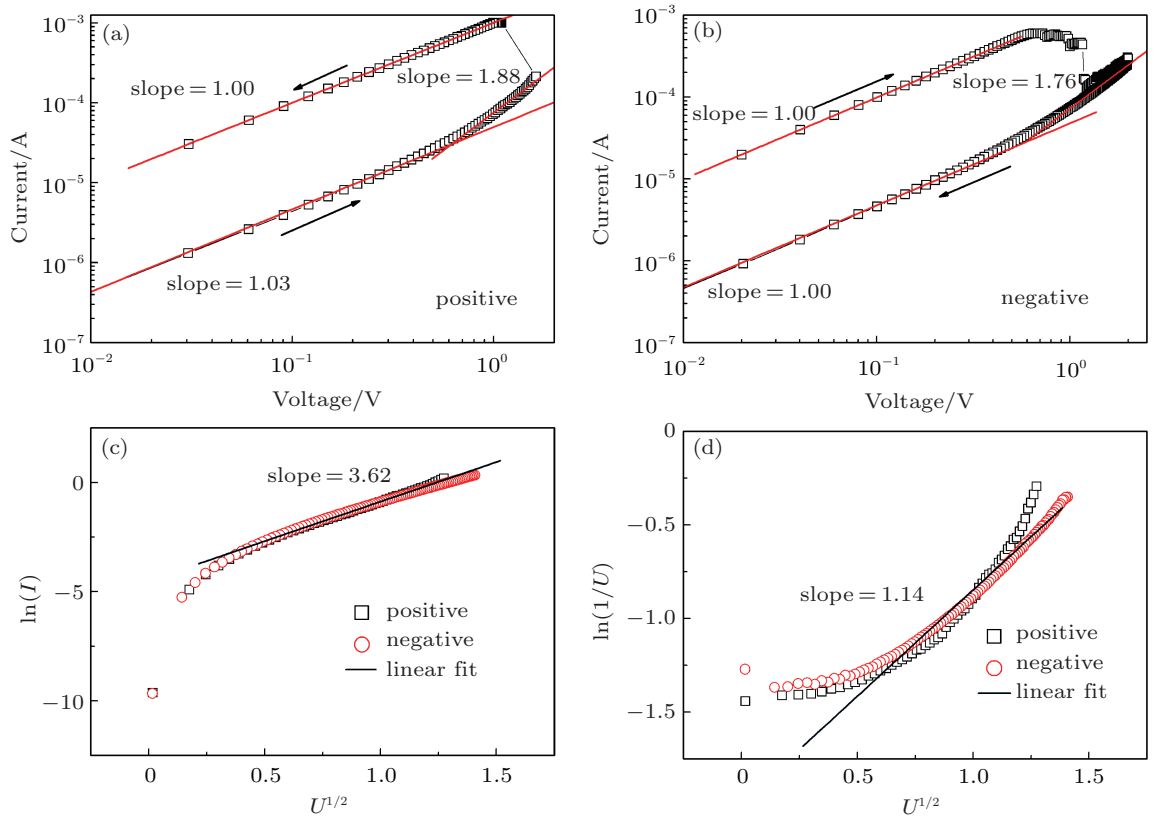


Fig. 3. (color online) Typical *I*–*V* characteristics in log–log scale of the LNO/BFZO/Pt structure with (a) positive voltage and (b) negative voltage, respectively. The *I*–*V* data in the HRS are fitted by (c) Schottky emission and (d) PF emission, respectively.

where ϕ is the height of Schottky barrier and K is the dielectric constant of the film. The third mechanism is PF emission, which is considered to be a common leakage mechanism in BFO film.[37,41] The bulk-limited PF emission involves the consecutive hopping of charges between defect trap centers. The conductivity for PF emission obeys[37,42]

$$\frac{I}{U} = \frac{J}{E} = \sigma_{\mathrm{PF}} = c \exp\left[\frac{E_1}{k_{\mathrm{B}}T} - \frac{1}{k_{\mathrm{B}}T}\left(\frac{q^3 U}{\pi\varepsilon_0 K d}\right)^{1/2}\right], \quad (3)$$

where c is a constant; E_1 is the trap ionization energy; k_{B} is the Boltzmann constant. The rather poor linear fit of $\log(I/U)$ versus $U^{1/2}$ [Fig. 3(d)] excludes the PF conduction mechanism. Quite good linear fitting of $\log(I)$ versus $U^{1/2}$ has been obtained at high field [Fig. 3(c)]; a dielectric constant of ~ 3.62 was obtained, which is comparable to the reported dielectric constant of 6.25 from the index of refraction of 2.5 for $BiFeO_3$ by Iakovlev *et al.*[43] Therefore, the Schottky emission also has contribution in the HRS state. As a result, conductive filaments and the Schottky barrier exist simultaneously during the resistive switching process.

In order to further study the origin of the resistive switching, we measured the impedance spectra after the forming process on different cells at room temperature. Figure 4 shows the impedance data of the HRS and LRS on log-scale in Cole–Cole form. It is obvious to see that the impedance spectrum of HRS consists of two semi-circles while only one semi-circle exists in that of LRS. The two semi-circles are attributed to film and interface contributions and usually fitted using RC elements.[44] In this regard, the resistance transition from HRS to LRS can be attributed to a broken Schottky barrier in the interface. The impedance spectra of HRS and LRS are fitted using the conventional RC elements with the equivalent circuits, as shown in Fig. 4. The RC elements correspond to charge transport either internal to the film or through the film interface. R_0 represents all the Ohmic resistance including wires for the measurement. The obtained parameters are summarized in Table 1. By assuming the parallel RC elements, the calculated data are in good agreement with the experimental impedance spectra. Note that the cells in the HRS and LRS measurements are not the same cell. It can be seen that the calculated R_1, C_1, and R_0 in HRS and LRS are similar. Combined with the I–V and impedance measurements, it can be seen that a high resistive layer emerges at the interface with the top Pt layer in the HRS.

Table 1. Summary of the equivalent circuit parameters by fitting the impedance spectra in the HRS and LRS.

Resistance state	R_1/Ω	C_1/F	R_2/Ω	C_2/F	R_0/Ω
HRS	107.4	1.55×10^{-10}	1.54×10^{5}	1.91×10^{-10}	268.3
LRS	356.5	1.74×10^{-10}	/	/	522.9

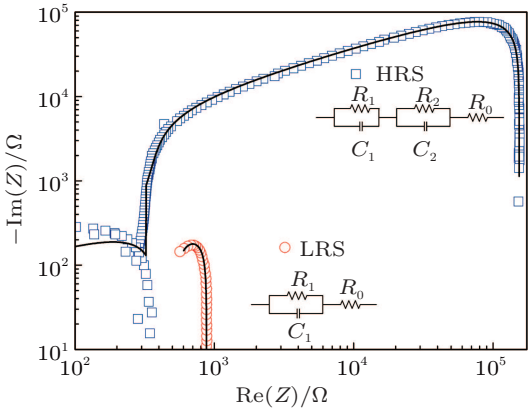


Fig. 4. (color online) Impedance data on log scale in Cole–Cole form in the HRS and LRS with fitting, respectively. Equivalent circuits are shown in the inset. Hollow symbols are experimental data and solid curves are results of fitting.

Mayer discussed the resistive switching characteristics in ferroelectric capacitors and proposed a 2-layer model with a conductive ferroelectric/interfacial dielectric layer sequence to explain the phenomenon.[45] As discussed before, the contact resistance at the epitaxial BFO/LNO interface is much lower than the one formed at the nonepitaxial Pt/BFO interface, so we consider only the interfacial layer at the Pt/BFZO interface. Based on the Schottky barrier model and considering the multiple steps of resistance change in the conducting filaments model, these two conduction mechanisms may simultaneously exist in our resistive switching device. Such a structure is shown in the schematic diagram in Fig. 5. The movement of oxygen vacancies in BFZO toward the surface has been reported to effectively lower the Schottky barrier height of the Pt top electrode, resulting in large conduction.[46] With positive voltage applied on the LNO layer, the oxygen vacancies will be pushed to the BFO/Pt interface and accumulate there. Thus, the conductive filaments will be formed. Furthermore, the Schottky barrier height has been effectively decreased. Thus, conductive filaments from LNO to Pt layers without an interfacial Schottky barrier have been formed, and only one semicircle can be observed in the impedance spectra. The device is switched to the LRS. With negative voltage applied on the LNO electrode, the oxygen vacancies will be tracked out from the BFO/Pt interface. The conductive filaments are broken, and the Schottky barrier height is increased. The device switches to the HRS, and rectifying I–V can be observed. Two semi-circles can be observed in the impedance spectra in the HRS. The formation/rupture of the conductive filaments mainly happens at the interface with the top Pt electrodes, which is widely used to explain the mechanism of the unipolar resistive switching (URS).[47,48] The polarity-dependent resistive switching might be due to the asymmetry of the bottom and top electrodes, and the formation of the Schottky barrier

at the top interface with the Pt electrodes.[49]

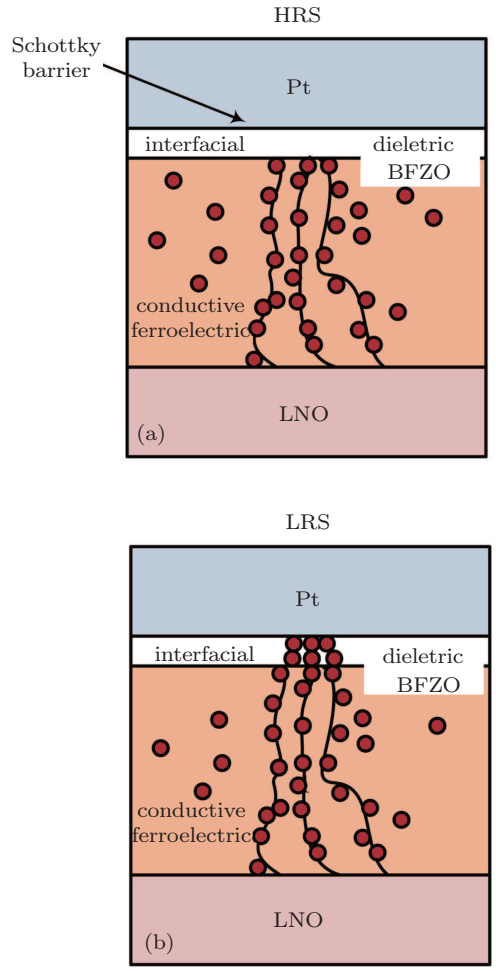


Fig. 5. (color online) Schematic diagrams of resistive switching mechanism: (a) HRS and (b) LRS.

4. Conclusions

In summary, BFZO films have been prepared by pulsed laser deposition on (001) STO substrate with LNO as buffer layer and bottom electrode, and Pt as top electrode. BRS with a resistive ratio of the HRS to the LRS of over three orders of magnitude has been observed. From the *I*–*V* characteristics, the conduction of the LRS is dominantly Ohmic, while the HRS is dominated by the SCLC together with Schottky emission at the BFZO/Pt interface. With the impedance spectra, 2-layer structure of conductive ferroelectric/interface dielectric layers has been suggested, and the resistive switching behavior is concluded to be due to the formation/rupture of conductive filaments in the interface dielectric layer close to the top Pt electrodes.

References

[1] Waser R and Aono M 2007 *Nat. Mater.* **6** 833
[2] Waser R, Dittmann R, Staikov G and Szot K 2009 *Adv. Mater.* **21** 2632
[3] Beck A, Bednorz J G, Gerber Ch, Rossel C and Widmer D 2000 *Appl. Phys. Lett.* **77** 139
[4] Moreno C, Munuera C, Valencia S, Kronast F and Obradors X 2010 *Nano Lett.* **10** 3828
[5] Yu S, Wu Y and Wong H S Philip 2011 *Appl. Phys. Lett.* **98** 103514
[6] You Y, So B, Hwang J, Cho W, Lee S S, Chung T, Kim C and An K 2006 *Appl. Phys. Lett.* **89** 222105
[7] Tsunoda K, Fukuzumi Y, Jameson J R, Wang Z, Griffin P B and Nishi Y 2007 *Appl. Phys. Lett.* **90** 113501
[8] Seong T, Choi K B, Seo I, Oh J, Moon J W, Hong K and Nahm S 2012 *Appl. Phys. Lett.* **100** 212111
[9] Mojarad S, Goss J, Kwa K, Zhou Z, Al-Hamadany R S, Appleby D R, Ponon N and O'Neill A 2012 *Appl. Phys. Lett.* **101** 173507
[10] Kwon D, Kim K M, Jang J H, Jeon J M, Lee M H, Kim G H, Li X, Park G, Lee B, Han S, Kim M and Hwang C S 2010 *Nat. Nanotechnol.* **5** 149
[11] Magyari-Köpe B, Tendulkar M, Park S, Lee H Dand Nishi Y 2011 *Nanotechnology* **22** 254029
[12] Li J, Ohashi N, Okushi H and Haneda H 2011 *Phys. Rev. B* **83** 125317
[13] Sun J, Jia C H, Li G Q and Zhang W F 2012 *Appl. Phys. Lett.* **101** 133506
[14] Wang J, Neaton J B, Nagaragan V, Ogale S B, Liu B, Viehland D, Vaithyanathan V, Schlom D G, Waghmare U V, Spaldin N A, Rabe K M, Wuttig M and Ramesh R 2003 *Science* **299** 1719
[15] Chu Y H, Martin L W, Holcomb M B, Gajek M, Han S J, He Q, Blake N, Yang C H, Lee D, Hu W, Zhan Q, Yang P L, Fraile-Rodrìuez A, Scholl A, Wang A X and Ramesh R 2008 *Nat. Mater.* **7** 478
[16] Yang S Y, Seidel J, Byrnes S J, Shafer P, Yang C H, Rossell M D, Yu P, Chu Y H, Scott J F, Anger J W, Martin L W and Ramesh R 2010 *Nat. Nanotechnol.* **5** 143
[17] Yang C H, Seidel J, Kim S Y, Rossen P B, Yu P, Gajek M, Chu Y H, Martin L W, Holcomb M B, He Q, Maksymovych P, Balke N, Kalinin S V, Baddorf A P, Basu S R, Scullin M L and Ramesh R 2009 *Nat. Mater.* **8** 485
[18] Shuai Y, Zhou S, Bürger D, Helm M and Schmidt H 2011 *J. Appl. Phys.* **109** 124117
[19] Li M, Zhuge F, Zhu X, Yin K, Wang J, Liu Y, He C, Chen B and Li R 2010 *Nanotechnology* **21** 425202
[20] Yin K, Li M, Liu Y, He C, Zhuge F, Chen B, Lu W, Pan X and Li R 2010 *Appl. Phys. Lett.* **97** 042101
[21] Wang C, Jin K, Xu Z, Wang L, Ge C, Lu H, Guo H, He M and Yang G 2011 *Appl. Phys. Lett.* **98** 192901
[22] Hu G D, Fan S H, Yang C H and Wu W B 2008 *Appl. Phys. Lett.* **92** 192905
[23] Park J M, Gotoda F, Nakashima S, Kanashima T and Okuyama M 2011 *Curr. Appl. Phys.* **11** S270
[24] Yuan X, Xue X, Zhang X, Wen Z, Yang M, Du J, Wu D and Xu Q 2012 *Solid State Commun.* **152** 241
[25] Yuan X, Xue X, Si L, Du J and Xu Q 2012 *Chin. Phys. Lett.* **29** 097701
[26] Zavaliche F, Yang S Y, Zhao T, Chu Y H, Cruz M P, Eom C B and Ramesh R 2006 *Phase Trans.* **79** 991
[27] Gutiérrez D, Foerster M, Fina I and Fontcuberta J 2012 *Phys. Rev. B* **86** 125309
[28] Miyazaki H, Goto T, Miwa Y, Ohno T, Suzuki H, Ota T and Takahashi M 2004 *J. Eur. Ceram. Soc.* **24** 1005
[29] Zhang J, Yang H, Zhang Q, Dong S and Luo J K 2013 *Appl. Phys. Lett.* **102** 012113
[30] Choi B J, Jeong D S, Kim S K, Rohde C, Choi S, Oh J H, Kim H J, Hwang C S, Szot K, Waser R, Reichenberg B and Tiedke S 2005 *J. Appl. Phys.* **98** 033715
[31] Kim K M, Choi B J and Hwang C S 2007 *Appl. Phys. Lett.* **90** 242906
[32] Yang Y C, Pan F, Liu Q, Liu M and Zeng F 2009 *Nano Lett.* **9** 1636
[33] Liu Q, Dou C, Wang Y, Long S, Wang W, Liu M, Zhang M and Chen J 2009 *Appl. Phys. Lett.* **95** 023501
[34] Yang T, Harn Y, Chiu K, Fan C and Wu J 2012 *J. Mater. Chem.* **22** 17071
[35] Yang H, Luo H M, Wang H, Usov I O, Suvorova N A, Jain M, Feldmann D M, Dowden P C, Felmann R F and Jia Q X 2008 *Appl. Phys. Lett.* **92** 102113
[36] Tsurumaki A, Yamada H and Sawa A 2012 *Adv. Funct. Mater.* **22** 1040
[37] Pabst G W, Martin L W, Chu Y H and Ramesh R 2007 *Appl. Phys. Lett.* **90** 072902

[38] Yang H, Jain M, Suvorova N A, Zhou H, Luo H M, Feldmann D M, Dowden P C, De Paula R F, Foltyn S R and Jia Q X 2007 *Appl. Phys. Lett.* **91** 072911
[39] Xu Q, Yuan X and Xu M 2012 *J. Supercond. Nov. Magn.* **25** 1139
[40] Ji Z, Mao Q and Ke W 2010 *Solid State Commun.* **150** 1919
[41] Wang C, Takahashi M, Fujino H, Zhao X, Kume E, Horiuchi T and Sakai S 2006 *J. Appl. Phys.* **99** 054104
[42] Wen Z, Shen X, Wu J, Wu D, Li A, Yang B, Wang Z, Chen H and Wang J 2010 *Appl. Phys. Lett.* **96** 202904
[43] Iakovlev S, Solterbeck C H, Kuhnke M and Es-Souni M 2005 *J. Appl. Phys.* **97** 094901
[44] Schmidt R, Eerenstein W, Winiecki T, Morrison F D and Midgley P A 2007 *Phys. Rev. B* **75** 255111
[45] Meyer R, Rodriguez Contreras J, Petraru A and Kohlstedt H 2004 *Int. Ferroelectrics* **64** 77
[46] Farokhipoor S and Noheda B 2012 *J. Appl. Phys.* **112** 052003
[47] Sawa A 2008 *Mater. Today* **11** 28
[48] Nagashima K, Yanagida T, Oka K and Kawai T 2009 *Appl. Phys. Lett.* **94** 242902
[49] Verrelli E, Tsoukalas D, Normand P, Kean A H and Boukos N 2013 *Appl. Phys. Lett.* **102** 022909